Molecular Crystals and Liquid Crystals
Publication details, including instructions for authors and subscription information:
http://www.tandfonline.com/loi/gmcl16

Localiztion in Molecular Solids

C. B. Duke [a]
[a] Xerox Corporation, Xerox Square-114, Rochester, N. Y., 14644, U.S.A.
Version of record first published: 21 Mar 2007.

To cite this article: C. B. Duke (1979): Localiztion in Molecular Solids, Molecular Crystals and Liquid Crystals, 50:1, 63-84

To link to this article: http://dx.doi.org/10.1080/15421407908084415

Mol. Cryst. Liq. Cryst., 1979, Vol. 50, pp. 63–84

Printed in Holland

Localization in Molecular Solids

C. B. DUKE

Xerox Corporation, Xerox Square—114, Rochester, N.Y. 14644, U.S.A.

(*Received 16 June, 1978*)

The local or extended nature of molecular ion or exciton states in molecular solids is determined by a competition between fluctuations in the local site energies of these states (which tend to localize them) and the hopping integrals for inter-site excitation transfer (which tend to delocalize them). This paper constitutes a brief survey of a body of work in which the parameters governing the localization of molecular ion states are evaluated spectroscopically with the aid of molecular orbital theory and subsequently utilized to assess the character of these states in a variety of molecular solids, including pendant-group polymers, Van der Waals crystals, and segregated-stack, quasi-one-dimensional charge transfer salts.

To illustrate the utility of this approach the example of electron localization in polystyrene (PS) and poly(2-vinyl pyridine)(PVP) is developed. Specifically, a model of electron interactions with longitudinal polarization fluctuations is described and shown to predict the (relaxation-energy) shifts and broadening of the photoemission lines from these polymers relative to those from the model molecules ethyl benzene and 2-vinyl pyridine, respectively. This example reveals the power of the methodology because the relaxation energy shifts in PS and PVP are identical although their low-frequency dielectric constants differ by a factor of two: a result which was unexplicable within the context of previous models of solvation in dielectric media.

Applications of the methodology to predict successfully extended states in segregated-stack charge transfer salts, relaxation-energy-induced surface states in Van der Waals solids, and a localized-extended state transition in Van der Waals crystals are indicated.

INTRODUCTION

In spite of considerable interest over the years in applications of polymers with controlled electrical and mechanical properties,[1] the qualitative nature of the electronic states in both polymers[2–4] and molecular crystals[5–8] remains a subject of controversy. The central issue[9] is whether these states are localized (e.g., molecular ion states) or extended (e.g., energy band states) in character. Our purpose in this paper is to present a brief overview of a body of recent work devoted to the spectroscopic characterization of polymers, molecular solids and molecules and to the utilization of the resulting data in an analysis of localization in certain pendant-group polymers,[9–11] Van der Waals solids,[7,9,10,12] and segregated-stack quasi-one-dimensional charge transfer salts.[8,13,14]

The central theme characteristic of this approach is the specification of the nature of electron and exciton states in molecular solids in terms of independently observable properties of the underlying molecular moieties and measured spectra (e.g., dielectric response) of the solids themselves. Appropriate gas-phase molecular species are characterized by photoemission spectroscopy (PES) and ultraviolet absorption spectroscopy (UVA).[11] The resulting molecular spectra are interpreted in terms of molecular cation and exciton states, respectively, which are in turn described by a spectroscopic CNDO molecular orbital model referred to as CNDO/S3 for aromatic hydrocarbons[15–18] and heterocycles thereof.[19] For molecules built of group V and VI atoms, a variant of this model is used which is called CNDO/S.[20,21] The energies, wave functions, and electron coupling constants to molecular vibrations of molecular cation and exciton states are extracted from these CNDO molecular orbital analyses of measured molecular PES and UVA spectra.

Polymeric and molecular solids are characterized by PES and the variety of spectroscopies which must be used to obtain a complete description of the dielectric response function, $\varepsilon(\mathbf{q}, \omega)$.[11] The measured $\varepsilon(\mathbf{q}, \omega)$ together with the CNDO/S3 wave functions suffice to define uniquely a model Hamiltonian describing electron and exciton interactions with longitudinal ("intermolecular") polarization fluctuations characteristic of molecular dielectrics.[11] The eigenstates of this Hamiltonian permit the evaluation of intermolecular contributions to the relaxation energies of injected charges (electrons, holes) and excitons in uniform dielectric media, as well as the dynamic fluctuations in these energies. These dynamic longitudinal polarization fluctuations lead to the homogeneous contributions to observed PES and UVA linewidths. In addition, however, surfaces, defects, and in polymers local compositional variations lead to inhomogeneous contributions to the observed linewidths.[9,10] These may be described by a tight-binding (Hückel) model in which the site energies (hopping integrals) are taken to vary from one site (pair of sites) to another. For example, in polymers the site energies may be described by (static) statistical distributions caused by the influence of local compositional variations on the relaxation energies of injected charges or excitons. These fluctuations in site energy may be evaluated in terms of simple models for surface energies and compositional variations. The resulting parameters are utilized to provide an analysis of the localized or extended character of the wave functions of injected charges or excitons in non-uniform molecular insulators.[10]

The major results of our examination of localization in molecular solids are that in polymers and molecular glasses static-polarization-induced site energy fluctuations in the bulk nearly always produce localized states whereas in molecular crystals usually only surface states are generated by this mech-

anism.[9-12] Dynamic fluctuations of both the site energies and hopping integrals occur in all molecular solids. These cause strongly temperature dependent scattering of extended (band-like) states in the segregated-stack, linear-chain quasi-one-dimensional charge transfer salts[8,13,14] and a dynamic hopping regieme leading to temperature insensitive mobilities at high ($T \gtrsim 100$ K) temperatures in many Van der Waals crystals.[5-7] They do not generate major (homogeneous) contributions to the widths of PES line spectra, however, because static site-to-site variations in the electronic contributions to the molecular cation relaxation energies lead to wide (inhomogeneously-broadened) lines for solid state ionizations.

This paper is organized to highlight the major concepts, models and measurements leading to these results. We proceed by considering molecular ion states in the next section followed by a description of (dynamic) longitudinal polarization fluctuations in the following one. These discussions set the stage for the development of a model of the interaction of molecular ions with dynamic polarization fluctuations and its use to evaluate the density of molecular cation states in molecular solids for comparison with PES data. A consideration of the criteria for localization ensues, including examples of the verification that PES line spectra from both molecular crystals and pendant-group polymers are inhomogeneously broadened by site-to-site variations in the electronic-polarization-induced cation relaxation energies. The paper concludes with a synopsis.

MOLECULAR ION STATES

Molecular photoemission (PES) and ultraviolet absorption (UVA) spectroscopies measure the properties of molecular ion states and excited states of neutral molecules, respectively. Specifically, if both the variation with electron and photon energies of the dipole matrix elements of electromagnetic field of the incident light wave and the existence of final-state resonances are neglected, then measured PES elastic-emission intensities, $I(E_k, h\nu)$, are proportional to the probability, $P(E)$, of obtaining a molecular ion state of binding energy $E = h\nu - E_k$. The incident photon and exit electron energies are designated by $h\nu$ and E_k, respectively. Consequently, the customary procedure[22] in molecular spectroscopy is to calculate $P(E)$ and compare this quantity directly with measured $I(E_k, h\nu)$ for fixed $h\nu$. This analysis scheme is not without difficulty. For example, in x-ray photoemission spectroscopy (XPS) the higher binding energy carbon-2s-derived molecular ion states of hydrocarbons are emphasized relative to 2p derived states whereas in ultraviolet photoemission spectroscopy (UPS) the converse is the case. If one recognizes these facts, however, comparisons of $I(E_k, h\nu)$ and $P(E)$ can be quite useful, so we shall utilize them herein.

A separate issue concerns the approximations utilized to calculate the energies and wave functions of molecular ion (or exciton) states.[22] For an isolated molecule, most molecular valence-electron cation states are comprised of an individual half-filled (nondegenerate) valence molecular orbital accompanied by distortions from their values in the neutral molecule both of the other occupied molecular orbitals and of the nuclear coordinates of the atomic constituents of the molecule. These distortions can be envisaged as the response of the other molecular coordinates to the charge density created by the vacated orbital. The energy gained by the molecular ion system upon undergoing such distortions relative to the neutral molecule state is called the *intra*molecular relaxation energy, E_r(intra), which in turn is divided into electronic (e) and atomic (a) contributions. If a molecule is embedded in a (solid or liquid) medium, then the charge density on the corresponding molecular ion induces analogous electronic and atomic distortions in the surrounding medium. These lead to the *inter*molecular contributions, E_{re}(inter) and E_{ra}(inter), respectively, to the relaxation energy. For typical molecular solids the total relaxation energy is $E_r \sim 4$–5 eV, roughly equally divided between *intra*molecular and *inter*molecular terms.[9] Since these values of E_r are quite large, we next must inquire into how they are incorporated into our analyses of PES spectra.

A complete evaluation of molecular ion eigenstates and eigenvalues involves first obtaining a good Hartree–Fock description of the ion and subsequently extending this description to include the influence of electron correlations by either configuration-interaction[22] or Green's function[23] methods. While such calculations are feasible for small (e.g., diatomic through tetratomic) molecules, our interest is centered around considerably larger molecules (e.g., S_8, Se_8, ethyl benzene) of interest in electrophotographic applications. Consequently, it was necessary to develop semi-empirical spectroscopic CNDO-level molecular orbital (MO) models which describe simultaneously the low-energy excited singlet states (molecular excitons) of the neutral species and the low-ionization-potential molecular ion states of the molecules of interest.[15–21] In these models the intramolecular electronic contributions to the relaxation energies, E_{re}(intra), are built into the molecular-orbital eigenvalues by construction. Stated differently, these models are perhaps best regarded as extrapolation procedures which permit the determination of the molecular ion and exciton states of complex molecules given a description of these states in simpler ones.

Given the semiempirical CNDO/S models, the molecular-ion-state probability density, $P(E)$, is evaluated by representing each orbital eigenvalue by a Gaussian of width $w \simeq 0.2$ eV which stimulates the experimental resolution of the PES instrument. A comparison of the calculated $P(E)$ for orthorhombic sulfur with measured gas-phase[24] and thin-film[25] UPS data is shown in

Figure 1. It is typical[26,27] of Van der Waals solids that the solid-state spectra replicate the gas-phase spectra but are broader and shifted to lower electron binding energies by an average intermolecular relaxation energy $\bar{E}_r(\text{inter}) \sim 1$–2 eV. Comparisons of calculated CNDO $P(E)$ with PES spectra have been performed for a wide variety of molecules, including substituted benzenes,[15,18] polyacenes,[15] paracyclophanes,[16] substituted polyenes,[17] nitrogen heterocycles,[19,28] oxygen heterocycles,[29] Se_8,[21] S_4N_4,[20] As_4S_4,[30] As_4Se_4,[30] As_4S_6,[27] and TCNQ.[31–33] The results in all cases are comparable to those shown in Figure 1 for S_8.

While intramolecular electronic contributions to the relaxation energy are incorporated *a priori* in the CNDO/S models, the intramolecular atomic contributions are evaluated by analysis of vibrational progressions in the PES spectra.[23,32–35] For the purpose of analyzing PES data, the important electron interactions with molecular vibrations are those which describe the modulation of molecular-ion-state energies by the symmetric modes of vibration of the ion.[34] Using the CNDO/S formalism, the linear electron-intramolecular-vibration coupling constants, $\{g_{\gamma i}\}$, for a molecular orbital labeled by γ are defined by expanding the orbital eigenvalues, E_γ, in terms of dimensionless vibrational normal mode coordinates, i.e.:

$$E_\gamma(\{Q_i\}) = E_\gamma(\{0\}) + \sum_i \left(\frac{\partial E_\gamma}{\partial Q_i}\right)_0 Q_i + \sum_{i,j}\left(\frac{\partial^2 E_\gamma}{\partial Q_i \partial Q_j}\right)_0 \frac{Q_i Q_j}{2} + \ldots \quad (1)$$

The normal coordinates Q_i are related to the lattice displacement vectors $\vec{u}_n = \vec{r}_n - \vec{r}_n^{(0)}$ by well-known relationships.[36] The linear terms in Q_i in Eq. (1) correspond to the linear electron-intramolecular-vibration interactions. The corresponding coupling constants are defined by writing Eq. (1) in second-quantized form[34]

$$H = \sum_\gamma E_\gamma(0) c_\gamma^+ c_\gamma + \sum_i \hbar\omega_i (b_i^+ b_i + 1/2) + \sum_{i,\gamma} g_{\gamma i} \hbar\omega_i c_\gamma^+ c_\gamma (b_i^+ + b_i) \quad (2)$$

in which i denotes the vibrational quantum modes, c_γ^+ and b_i^+ are the creation operators associated with the electronic orbital and vibration quanta of energies E_γ and $\hbar\omega_i$, respectively, and the $\{g_{\gamma i}\}$ are the desired dimensionless linear electron-intramolecular-vibration coupling constants given by

$$g_{\gamma i} = \frac{1}{\sqrt{2\hbar\omega_i}}\left(\frac{\partial E_\gamma}{\partial Q_i}\right)_0. \quad (3)$$

An important property of Hamiltonian (2) is that it can be solved exactly,[37] thereby providing a simple analytical form for the intensity distribution in the vibrational structure associated with transitions between eigenstates of the Hamiltonian (2). In addition, the lowering in energy of a given orbital

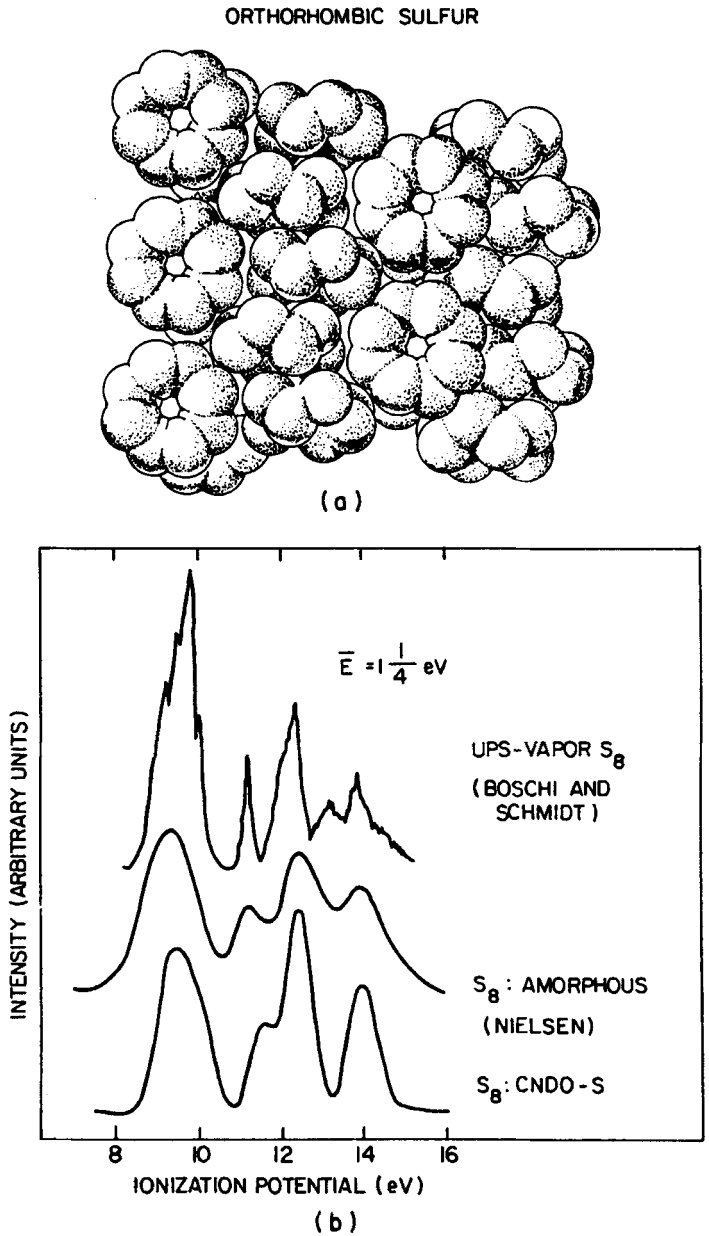

FIGURE 1 Diagram of the structure of orthorhombic sulfur and a comparison in Panel (b) of gas phase UPS data,[24] solid-state UPS data,[25] and the calculated valence electron density of states of S_8.[21] $\bar{E}$ designates the shift (to lower binding energy) of the solid-state relative to the gas phase UPS data. [After Duke.[9]]

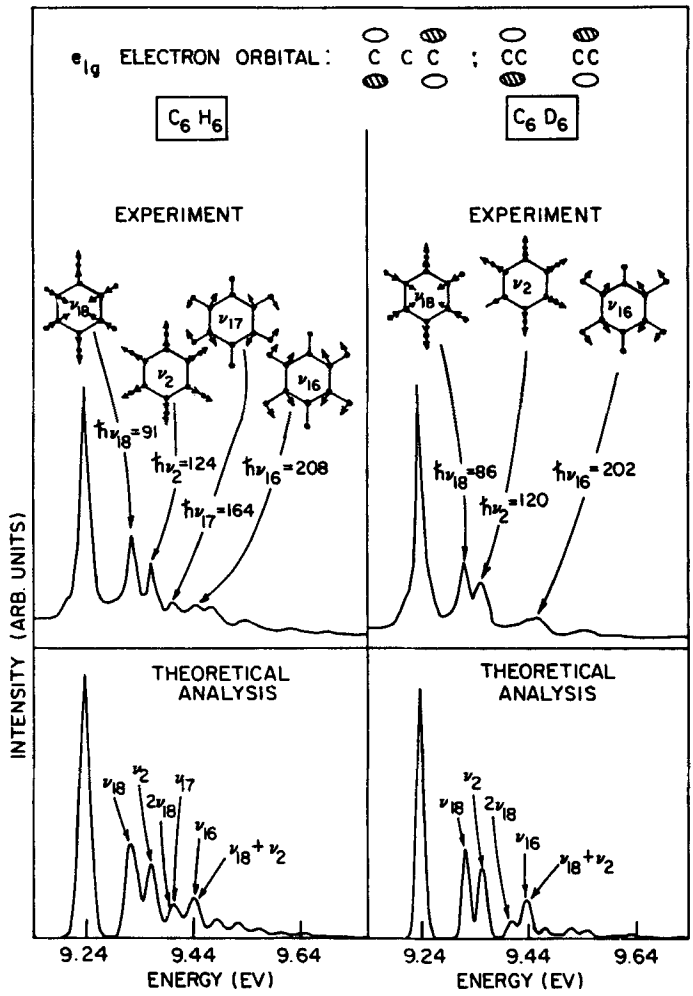

FIGURE 2 Comparison of observed (upper panels) and calculated (lower panels) vibration assisted photoemission from the $1e_{1g}(\pi)$ orbital of benzene (left-hand column) and deuterobenzene (right-hand column). The symmetry of the electronic orbitals is indicated at the top of the figure following the notation of Lindholm.[39] The symmetries and energies (in meV) of the molecular vibrations are indicated in the upper panels. The experimental spectra in the upper panel are those of Potts *et al.*[40] The interpretation of the lineshapes is indicated for the theoretical curves in the lower panels. The empirical values of the coupling constants are $g(\nu_{18}) = 0.60$, $g(\nu_2) = 0.53$, $g(\nu_{17}) = 0.28$, $g(\nu_{16}) = 0.26$ for benzene and $g(\nu_{18}) = 0.60$, $g(\nu_2) = 0.53$, $g(\nu_{17}) = 0.0$, and $g(\nu_{16}) = 0.26$ for deuterobenzene. The molecular vibration energies were taken directly from the experimental spectra. [After Duke and Lipari.[35]]

γ due to its interaction with the molecular vibrations, which is the atomic contribution to the intramolecular relaxation energy of a molecular ion in the state labeled by γ, may be evaluated explicitly in terms of the $g_{\gamma i}$, i.e.,

$$E_{ra}(\gamma, \text{intra}) = \sum_i g_{\gamma i}^2(\hbar\omega_i). \tag{4}$$

Consequently once the $\{g_{\gamma i}\}$ are obtained (e.g., by analysis of the intensities of PES vibrational progressions[34,35]) the atomic contribution to the intramolecular relaxation energies may be evaluated directly using Eq. (4).

Two qualitatively different approaches may be taken to evaluate the coupling constants $\{g_{\gamma i}\}$.[38] In the empirical approach they are obtained by fitting observed photoemission spectra using the $\{g_{\gamma i}\}$ as adjustable parameters. In the microscopic approach they are evaluated by using a molecular orbital model for the $E_\gamma(\{Q_i\})$ and a force field model for the $\{Q_i\}$. In the former approach, an analytical form for the ion-state density $P(E)$, obtained[34,37] from the eigenstates of the Hamiltonian given by Eq. (2), is utilized to describe the PES spectra. Typical results[34,39,40] for benzene and deuterobenzene are illustrated in Figure 2. The calculated values of the $\{g_{\gamma i}\}$ obtained using the CNDO/S model agree well with those obtained from the empirical approach.[34,35] Moreover, the CNDO/S microscopic approach is useful even when the empirical approach fails (e.g., due to inadequate resolution of the vibrational progressions[32,33]). A complete review of the published calculations and data analysis is given elsewhere.[38] Here, we conclude by observing that both the shape of the PES vibrational progressions and the magnitudes of $E_{ra}(\text{intra}) \sim 0.1$–$0.3$ eV are readily obtainable either from PES data directly or from suitable molecular-orbital and valence-force-field models.

POLARIZATION FLUCTUATIONS IN DIELECTRIC MEDIA

Turning to a consideration of the intermolecular contributions to the molecular ion relaxation energy, we recall that these arise from the electronic and atomic response induced in neighboring molecular species when an ion state is generated (e.g., by photoemission) on a particular molecule. A wide variety of models have been proposed in the literature for the evaluation of intermolecular relaxation induced by injected charges.[41] Since the similarity of the gas-phase and solid-state PES data [e.g., Figure 1] for the materials of interest to us suggest that for them photon-generated valence electron holes are molecular cation states, we describe in the following section a model based upon treating the surroundings of a particular molecular ion as a dielectric medium. This section is devoted to a recapitulation of the major features of our description of this medium.

The response of a dielectric medium to an injected charge is described by the coupling of that charge to the dynamic longitudinal polarization fluctuations in the medium. The energy-momentum relations, $E_\alpha(\mathbf{q})$, of these fluctuations are defined by

$$\varepsilon[E_\alpha(\mathbf{q}), \mathbf{q}] = 0 \tag{5}$$

in which $\varepsilon(\hbar\omega, \mathbf{q})$ is the dielectric function of the medium. We assume an isotropic medium for simplicity in our discussion. Both atomic and electronic relaxations are embodied in this model by virtue of the existence of atomic as well as electronic branches of longitudinal polarization fluctuations labeled by different values of α. In the special cases of polystyrene ["PS"] and poly-(2-vinyl pyridine) ["PVP"] a detailed model of $\varepsilon(E, \mathbf{q})$ has been developed elsewhere. For these materials four broad classes of polarization fluctuation occur. The low-frequency, $f \lesssim 10^5\ \text{sec}^{-1}$, fluctuations are associated both with motions of the polymer chain and with torsional motions of the pyridine moiety relative to the hydrocarbon backbone. The infrared response, $10^{12}\ \text{sec}^{-1} \lesssim f \lesssim 10^{14}\ \text{sec}^{-1}$, is caused by infrared active modes of the pyridine moiety[18,56] modified by coupling to the hydrocarbon backbone. The UV response, $10^{15}\ \text{sec}^{-1} \lesssim f \lesssim 10^{16}\ \text{sec}^{-1}$, is generated by particle-hole ("exciton") excitations of the valence electrons whereas the far UV response, $f \gtrsim 6 \times 10^{17}\ \text{sec}^{-1}$ is associated with analogous excitations of the C and N $1s$ core electrons. Since the core excitations contribute an amount to the dielectric function which is negligible relative to that of the valence electrons, we ignore them. The form used for the dielectric function is given by:[11]

$$\varepsilon(E, \mathbf{q}) = 1 + \sum_{\alpha=1}^{4} \frac{E_{p\alpha}^2}{\Delta_\alpha^2(\mathbf{q}) - E^2}, \tag{6a}$$

$$\Delta_\alpha(\mathbf{q}) = \Delta_\alpha[1 + \Lambda_\alpha^2 q^2] + i\Gamma_\alpha, \tag{6b}$$

$$\Delta_1 \sim 10^{-13}\ \text{eV}; \Lambda_1 \sim 10\ \text{Å (torsional modes)}, \tag{7a}$$

$$\Delta_2 \sim 10^{-2}\ \text{eV}; \Lambda_2 \sim 5\ \text{Å (IR modes)}, \tag{7b}$$

$$\Delta_3 \sim 10\ \text{eV}; \Lambda_3 \sim 1\ \text{Å (valence-electron modes)}, \tag{7c}$$

$$\Delta_4 \sim 300\ \text{eV}; \Lambda_4 \sim 0.1\ \text{Å (core-electron modes)}. \tag{7d}$$

The values of $E_{p\alpha}$, Δ_α and Γ_α are determined by fitting measured dielectric response data. A model in which a single oscillator is used to describe each type of branch of the fluctuation spectrum (i.e., torsional, IR, and valence-electron modes, respectively) is indicated in Figure 3, in which comparisons with measured dielectric response data are shown as insets.

A detailed discussion of the determination of the parameters in Eqs. (6) and (7) is given by Duke *et al.*[11] For our present purposes it suffices to note

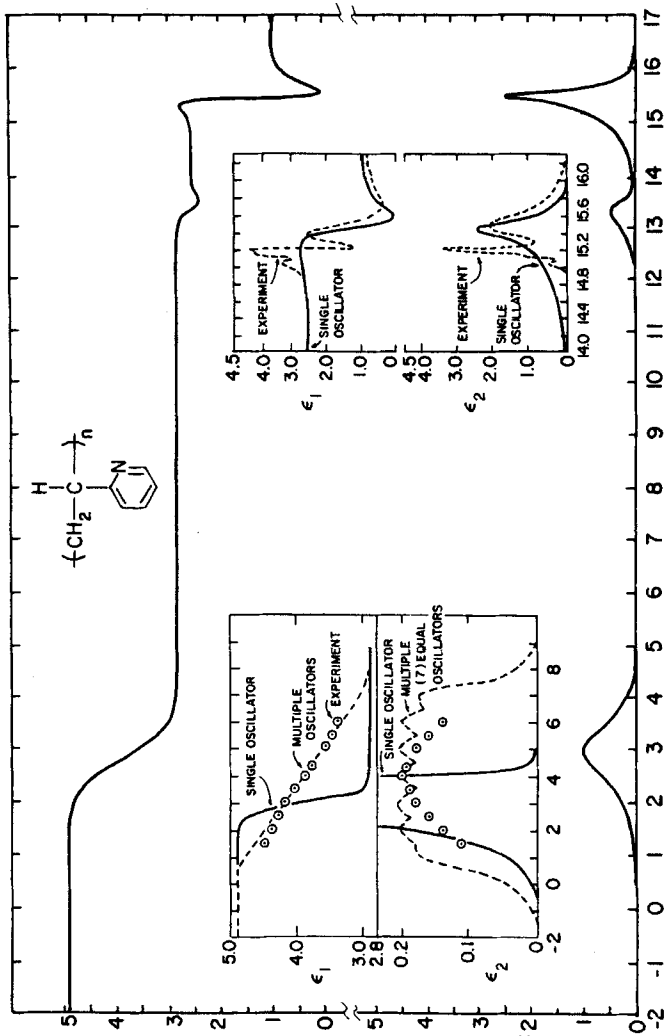

FIGURE 3 Plot of the model dielectric response of poly(2-vinyl pyridine), as a function of frequency, f, in cycles/sec. The insets show comparisons with the experimental data in the low frequency and ultraviolet energy regions. No quantitative dielectric response data are available in the IR region. [After Duke *et al.*[11]]

that the various branches of the longitudinal polarization fluctuation spectrum can make quantitatively different types of contribution to the PES spectrum. Therefore in the following section we use the dielectric function shown in Figure 3 to illustrate this important result.

ELECTRON COUPLING TO DYNAMIC LONGITUDINAL POLARIZATION FLUCTUATIONS

Given the expressions for $\varepsilon(E, \mathbf{q})$ and $E_\alpha(\mathbf{q})$ specified by Eqs. (5) and (6), a universal Hamiltonian describing the motion of an injected charge in a (uniform) dielectric medium can be written as:[11]

$$H = H_e + \sum_{\alpha,\mathbf{q}} V_\alpha(\mathbf{q})[b_\alpha^+(\mathbf{q})\rho(-\mathbf{q}) + b_\alpha(\mathbf{q})\rho(\mathbf{q})] + \sum_{\alpha,\mathbf{q}} E_\alpha(\mathbf{q})[b_\alpha^+(\mathbf{q})b_\alpha(\mathbf{q}) + \tfrac{1}{2}], \tag{8a}$$

$$V_\alpha(\mathbf{q}) = [2\pi e^2 E_{p\alpha}^2/\mathbf{q}^2 E_\alpha(\mathbf{q})]^{1/2} \tag{8b}$$

$$H_e = \sum_{i,\gamma} \varepsilon_{\gamma i} c_{i\gamma}^+ c_{i\gamma} + \sum_{\substack{i\neq j \\ \gamma,\delta}} V_{ij}^{\gamma\delta} c_{j\delta}^+ c_{i\gamma} = \sum_\lambda E_\lambda c_\lambda^+ c_\lambda, \tag{8c}$$

$$\rho(\mathbf{q}) = \sum_{\lambda',\lambda} c_{\lambda'}^+ c_\lambda M_{\lambda'\lambda}(\mathbf{q}), \tag{8d}$$

$$M_{\lambda'\lambda}(\mathbf{q}) = \int d^3r \bar{\phi}_{\lambda'}(\mathbf{r})\phi_\lambda(\mathbf{r}) \exp(-i\mathbf{q}\cdot\mathbf{r}). \tag{8e}$$

The c_λ are the annihilation operators of the electrons in the eigenstate of H_e labeled by λ, i.e., possessing an eigenvalue E_λ and eigenfunction $\phi_\lambda(\mathbf{r})$. The $c_{i\gamma}$ are the annihilation operators of electrons in the site representation associated with a site index i and molecular orbital index γ. Thus, γ designates the isolated molecular ion states characterized by gas-phase PES measurements and the CNDO/S models. The $b_\alpha(\mathbf{q})$ are the annihilation operators of the longitudinal polarization fluctuations whose energy $E_\alpha(\mathbf{q})$ is given by Eq. (5). The V_{ij} in Eq. (8c) are the intersite hopping integrals between molecular ion sites in the solid. Finally, the $V_\alpha(\mathbf{q})$ given in Eq. (8b) are the electron-polarization-fluctuation coupling functions. Eqs. (8) together with Eqs. (5)–(7) describing the computation of the energies, $E_\alpha(\mathbf{q})$, of the longitudinal polarization fluctuations define completely the model of a molecular anion, cation or exciton at a molecular site interacting both with those on other sites (via the V_{ij}) and with the (longitudinal) polarization fluctuations of the surrounding dielectric medium.

To proceed further, we must know the eigenvalues $\{E_\lambda\}$ and eigenfunctions $\{\phi_\lambda\}$ of the electronic Hamiltonian, H_e. We argue in the following

section that static polarization fluctuations localize low-energy electrons and holes at individual molecular ion sites to form molecular anions and cations, respectively. Consequently, we take the $\{\phi_\lambda\}$ as the molecular orbitals of these molecular ions. Since the $\{\phi_\lambda\}$ are orthogonal we see that $M_{\lambda'\lambda}(\mathbf{q} = 0)$ vanishes if the site indices are the same and the orbital indices are not. For interpretations of the UPS data it suffices to neglect the intersite hopping integrals so that $\lambda = (i, \gamma)$ and

$$M_{i\gamma,j\beta}(\mathbf{q}) = \delta_{ij}\delta_{\gamma\beta} \exp[-i\mathbf{q} \cdot \mathbf{R}_j] f_\gamma(\mathbf{q}), \tag{9a}$$

$$f_\gamma(\mathbf{q}) = \int d\mathbf{r}^3 e^{-i\mathbf{q}\cdot\mathbf{r}} |\phi_\gamma(\mathbf{r} - \mathbf{R}_j)|^2 \tag{9b}$$

in which $\mathbf{R}_j$ is a vector to the origin associated with the site labeled by j.

The important consequence of these considerations resides in the result that in the independent-ion limit defined by Eqs. (9), $M_{\lambda'\lambda}(\mathbf{q})$ is diagonal in λ. Hence, the Hamiltonian given by Eqs. (8) can be diagonalized by canonical transformation.[37] This procedure eliminates the electron-fluctuation coupling term linear in $V_\alpha(\mathbf{q})$ in Eqs. (8) and gives the intermolecular contributions to the relaxation energy as the change in zero-point energy of the polarization fields created by the extra charge in the molecular orbital labeled by γ, i.e.,

$$E_r(\gamma, \text{inter}) = \sum_{\mathbf{p},\alpha} g_\gamma^2(\mathbf{q}, \alpha) E_\alpha(\mathbf{q}), \tag{10a}$$

$$g_\gamma^2(\mathbf{q}, \alpha) = |V_\alpha(\mathbf{q}) f_\gamma(\mathbf{q}) / E_\alpha(\mathbf{q})|^2. \tag{10b}$$

For our present purpose of illustrating the qualitatively different consequences on the PES spectra of different branches of the polarization fluctuation spectrum, we can treat the molecular ion states as spherical charge densities of radius R to get effective coupling constants integrated over $\mathbf{q}$, i.e.[11]

$$g_R^2(\alpha) = \left[\frac{E_{p\alpha}}{E_\alpha(0)}\right]^2 \frac{e^2}{2RE_\alpha(0)}. \tag{11a}$$

In this model the zero-point energy expression for the relaxation energy, Eqs. (10), becomes

$$\begin{aligned} E_r(R, \text{inter}) &= \sum_\alpha g_R^2(\alpha) E_\alpha(0) \\ &= \sum_\alpha E_r(R, \alpha, \text{inter}). \end{aligned} \tag{11b}$$

The spherical charge model is suggested by PES data like those shown in Figure 1 because all of the molecular ion states are shifted in energy by the same amount in the solid state relative to the gas phase. Consequently, the

details of their wave functions cannot be important in evaluating the intermolecular contributions to the relaxation energy.

We now arrive at a crucial step of our analysis. Eqs. (10) and (11) presuppose that the molecular-ion-state-induced change in the zero-point energy of the polarization field, a quantity which emerges from the diagonalization of the Hamiltonians given by Eqs. (2) or (8), is observed in PES. But a proper calculation of the molecular ion spectral density $P(E)$ reveals that such is not the case.[11,42] Rather it is necessary to distinguish between polarization fluctuations (or intramolecular modes, see Eqs. (2)–(4), Figure 2) which exhibit weak ($g_\gamma^2(\alpha) \ll 1$) and strong ($g_\gamma^2(\alpha) \gg 1$) coupling to a particular molecular ion state labeled by γ. Those fluctuations which exhibit weak coupling contribute to the intermolecular relaxation energy observed in PES whereas those which exhibit strong coupling lead to a homogeneous broadening of the PES ionization line associated with the state γ.

This important result is derived elsewhere.[11,42,43] Its physical interpretation is simple. The exact eigenstates of the coupled molecular-ion/polarization-fluctuation system consist of the molecular ion sharing its energy with fluctuations which co-exist with it. One such eigenstate consists of the molecular ion having all of the energy and the fluctuations none. If this state is excited with the highest probability in PES, than the relaxation energy shift given by Eqs. (4), (10) or (11) is observed. Such is the case, however, only if $g_\gamma^2(\alpha) < 1$, i.e., the molecular ion state γ is weakly coupled to the αth branch of the fluctuation spectrum. If $g_\gamma^2(\alpha) \gg 1$, then the most probable eigenstate of the coupled system is that in which the molecular ion shares precisely an amount $E_r(\gamma, \alpha, \text{inter})$ of energy with the fluctuations. Thus, when this state is observed in PES, it appears to have a higher binding energy by an amount $E_r(\gamma, \alpha, \text{inter})$ because this energy is generated by exciting polarization fluctuations of the medium when the ion is created. This additional energy required to excite the polarization fluctuations exactly cancels the relaxation energy shift of the zero-fluctuation line, yielding a broad-band spectrum centred at the unperturbed molecular ion energy. Calculation of the rms width, $\sigma_r(\gamma)$, of this band using the same approximations which led to Eq. (11b) for $E_r(R, \text{inter})$ gives[11]

$$\sigma_r^2(R) = \sum_\alpha \sigma_R^2(\alpha);\ g_R^2(\alpha) \gg 1 \tag{12a}$$

$$\begin{aligned}\sigma_R^2(\alpha) &= \tfrac{1}{2} g_R^2(\alpha) E_\alpha^2(0) \coth[E_\alpha(0)/2\kappa T)] \\ &= \tfrac{1}{2} E_r(R, \alpha) E_\alpha(0) \coth[E_\alpha(0)/2\kappa T)]\end{aligned} \tag{12b}$$

in which T designates the temperature and κ is Boltzman's constant. More complicated formulae govern the lineshapes when $g_R^2(\alpha) \sim 1$ as discussed by Duke *et al.*[11]

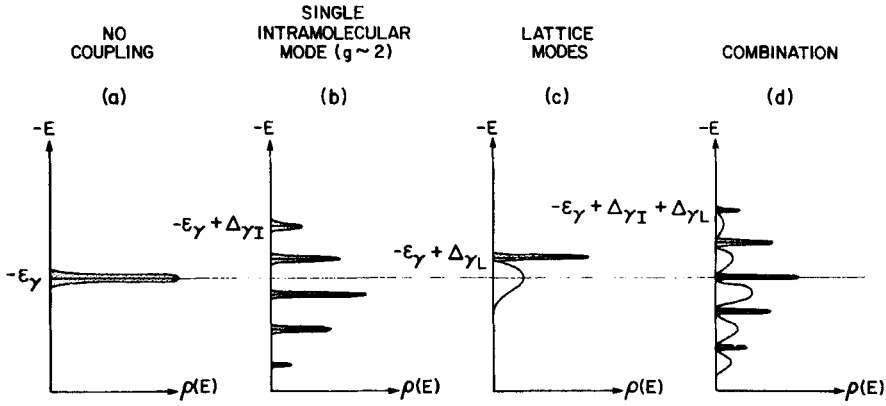

FIGURE 4 Schematic indication of the molecular ion spectra density, $\rho(E)$, associated with an orbital in a rigid molecule [panel (a)] coupled to a discrete (e.g., intramolecular) mode [panel (b)], coupled to a continuum of modes [panel (c)], and coupled to both the discrete and continuum models [panel (d)]. [After Duke.[42]]

To illustrate the general situation we show in Figure 4 a schematic diagram characteristic of intermediate coupling to an intramolecular fluctuation and weak coupling to continuum lattice fluctuations in a molecular crystal. As is evidence from the figure, the energy centroid

$$E_1 = \int P(E)EdE = E_r \tag{13}$$

is invariant under changes in electron-fluctuation coupling. The detailed shape of $P(E)$ depends, however, upon all the parameters describing the eigenstates of the Hamiltonians given by Eqs. (2) or (8), as described elsewhere.[11,34,42,43] Consequently, detailed analysis of PES data requires a knowledge of these parameters.

LOCALIZATION IN MOLECULAR INSULATORS

Having assembled the requisite background concepts we now turn to our main topic: a consideration of the nature of the eigenstates of excess holes (or electrons, if appropriate) injected into molecular insulators. The Hamiltonian on which we base our discussion has been given in Eq. (8c). Three central concepts underlie our analysis.[9] First, in molecular insulators the electronic site energies, $\{\varepsilon_{\gamma l}\}$ in Eq. (8c), form a distribution due both to their dynamic modulation by longitudinal polarization fluctuations and their static modulation due to surfaces, defects, and local compositional variations. Second, the transfer (or "hopping") integrals, $\{V_{ij}\}$ in Eq. (8c) also form a

distribution for similar reasons. Third, localization occurs when these fluctuations are sufficiently severe that they overcome the delocalization effect of the average hopping integrals

$$\bar{V} = \langle V_{ij} \rangle_{AV}. \tag{14a}$$

This problem has been studied mathematically for many years using lattice-gas models in which electronic motion on a lattice characterized by various hypothetical static random distributions of $\{\varepsilon_i\}$ and $\{V_{ij}\}$ is examined.[44] Roughly speaking, if we consider the first moments of these distributions

$$\Delta^2 \equiv \langle (\varepsilon_i - \bar{\varepsilon})^2 \rangle_{AV} \tag{14b}$$

$$(\Delta V)^2 \equiv \langle (V_{ij} - \bar{V})^2 \rangle_{AV} \tag{14c}$$

only localized states are obtained if

$$\Delta > c\bar{V} \tag{15}$$

in which c is a constant of the order of the dimensionality of the system times the coordination number of a given site.[45,46] Fluctuations in $\{V_{ij}\}$ cannot by themselves induce complete localization.[46,47] They can in effect reduce the value of c in Eq. (15), however, if present together with fluctuations in the $\{\varepsilon_i\}$.

An application of these mathematical results to predict the nature of electronic states in molecular solids has been given earlier.[9] For Van der Waals crystals we expect that electronic polarization fluctuations give $E_r(\text{inter}) \gtrsim 1$ eV whereas $\bar{V} \lesssim 0.1$ eV. Moreover, variations in $E_r(\text{inter})$ at surfaces lead to static fluctuations $\Delta \sim E_r(\text{inter})/4 > c\bar{V}$. This fact has two interesting consequences. First, the combination of surface-induced relaxation energy variations and the short inelastic-collision mean free paths, λ_e, for electrons photostimulated by UV light lead immediately to the prediction[10] of inhomogeneously broadened UPS lines: a result illustrated in Figure 5 for TNCQ,[9,31,48] and widely observed experimentally.[10] Moreover, in the limit that $\lambda_e \lesssim d_\perp$, where $d_\perp$ is the intermolecular layer spacing normal to the surface, it was predicted[9,10] that surface states should be observed because $\Delta > c\bar{V}$. Such states subsequently were observed in anthracene films,[12] as illustrated in Figure 6, by the disappearance of the high binding energy peak in $I(E_k, h\nu)$ at glancing angle take-off (i.e., $\theta = 80°$). These experiments also permitted the direct measurement of $E_r(\text{bulk; inter}) = 1.5 \pm 0.1$ eV as opposed to $E_r(\text{surface, inter}) = 1.2 \pm 0.1$ eV, in accordance with theoretical expectations.[9,10]

Another significant application of these concepts has been the determination of the nature of photostimulated molecular cation states in pendant-group polymers, specifically polystyrene ("PS") and poly(2-vinyl pyridine)

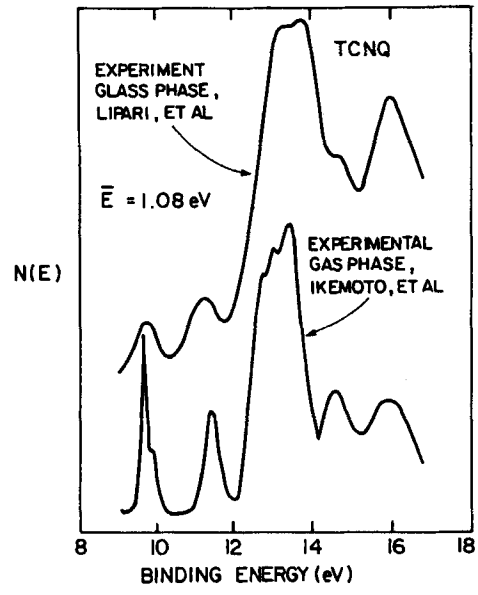

(a)

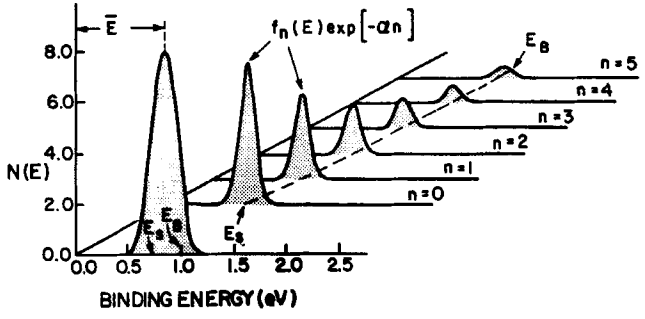

(b)

FIGURE 5 Panel (a): comparison of the solid state[31] and gas phase[48] UPS data of 7,7,8,8-tetracyano-p-quinodimethane. $\bar{E}$ designates the shift (to lower binding energy) of the solid-state relative to the gas-phase UPS data. Note the increased broadening of the ionization peaks in the solid-state relative to the gas-phase data. Panel (b): computation of the observed solid-state UPS ionization peak, $N(E)$, of a gas phase line represented by $f(E)$ which has been shifted in the solid state by an amount $\Delta E_n = [E_B - (E_B - E_S)\exp(-\beta n)]$ for a molecule in the layer at depth nd from the surface, where d is the layer spacing. Contributions from deeper layers are weighted by $\exp[-\alpha n]$. $\alpha = \beta = 0.5$, because of the inelastic collision damping of electrons elastically photo-emitted from molecules in these layers. [After Duke.[9]]

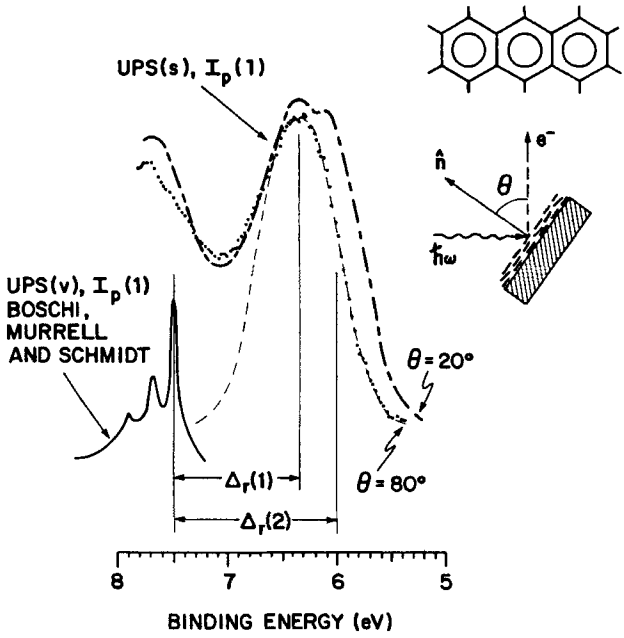

FIGURE 6 The high-resolution HeI UPS(s) angle-dependent data on $I_p(1)$ of anthracene are shown. For clarity, the $\theta = 20°$ data are approximately normalized to the peak intensity of the $\theta = 80°$ data at about 6.3-eV binding energy. $I_p(1)$ from Boschi *et al.*[49] is shown for determination of the top-layer relaxation energy, $\Delta_r(1) = 1.2 \pm 0.1$ eV and the subsequent layer value, $\Delta_r(\eta \geq 2) = 1.5 \pm 0.1$ eV. [After Salaneck.[12]]

("PVP").[11] In these cases, the molecular nature of photostimulated low-energy exciton and cation states is immediately evident upon comparison of the gas phase and polymer UVA and UPS spectra as shown in Figures 7–9. The remarkable result evident in Figures 8 and 9, however, is that the measured relaxation energies, $\bar{E}_r$, are identical for PS and PVP, despite a difference by a factor of about 2 in their static dielectric constants. The Born model of solvation, which is identical to Eqs. (10) for a spherical molecular ion charge density, predicts that

$$E_r(R, \text{inter}) = \frac{e^2}{2R}\left[1 - \frac{1}{\varepsilon(0, 0)}\right]. \tag{16}$$

Eqs. (11) and (16) lead to the expectation[11] that E_r for PVP should be about 4.5 eV relative to a value of about 1.3 eV for PS: a prediction in marked disagreement with the result that $E_r(\text{inter}) = 1.5 \pm 0.1$ eV for both polymers as shown in Figures 8 and 9. The theory described in the preceeding section of electron interactions with polarization fluctuation accounts for the experimental observations in a straightforward manner.[11] The coupling constants

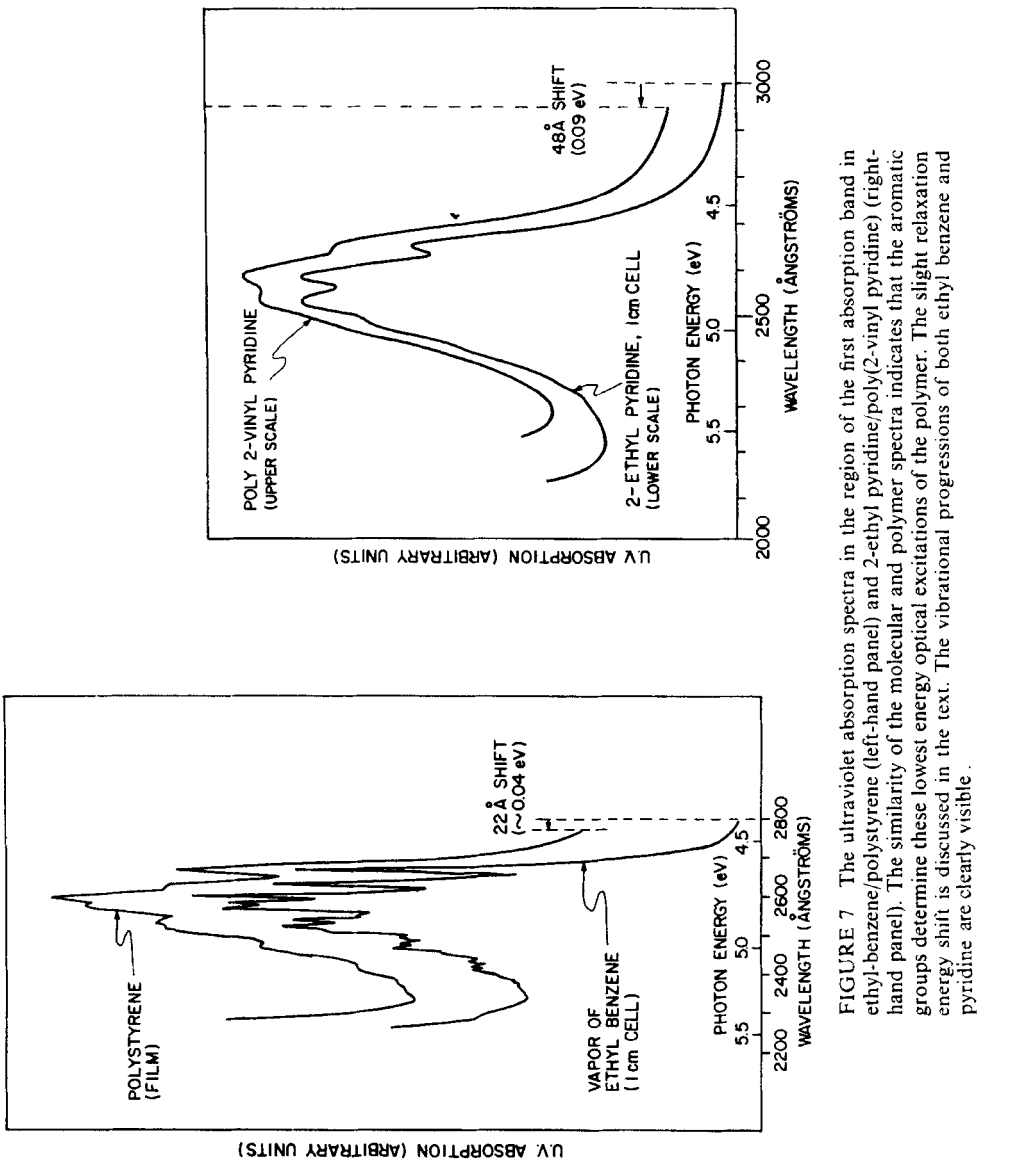

FIGURE 7 The ultraviolet absorption spectra in the region of the first absorption band in ethyl-benzene/polystyrene (left-hand panel) and 2-ethyl pyridine/poly(2-vinyl pyridine) (right-hand panel). The similarity of the molecular and polymer spectra indicates that the aromatic groups determine these lowest energy optical excitations of the polymer. The slight relaxation energy shift is discussed in the text. The vibrational progressions of both ethyl benzene and pyridine are clearly visible.

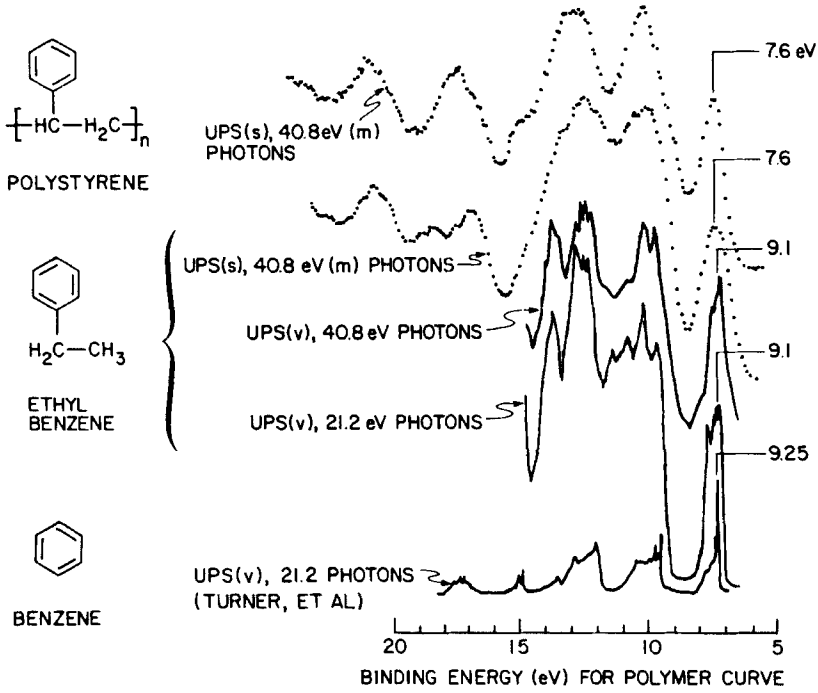

FIGURE 8 UPS data for the series of materials benzene(v),[50] 2-ethyl benzene(v), 2-ethyl benzene(s), and polystyrene(s). The shift of 0.14 eV between the lowest-binding-energy peak for benzene and the 2-ethyl benzene reflects the effects of hyperconjugation induced by the ethyl group substituent. The additional shift of 1.5 eV between the vapor(v) and solid-state(s) spectra on 2-ethyl benzene arises from the intermolecular relaxation effects discussed in the text. The spectra are presented in the figure shifted relative to each other by an amount such that the lowest-energy ionization potentials are aligned. The absolute values of these ionization potentials are indicated in the figure. [After Duke *et al.*[11]]

$g_\gamma^2(\alpha)$ given by Eq. (11a) are much greater than unity for the lower frequency torsional and *IR* longitudinal polarization modes which lead to the increase in $\varepsilon(E, 0)$ by a factor of over two from $E \sim 1$ eV to $E = 0$ (see, e.g., Figure 3). Therefore these polarization fluctuations homogeneously broaden the UPS lines rather than shift them. Since the electronic contributions to $\varepsilon(E, \mathbf{q})$ are essentially identical for PS and PVP, the measured $\bar{E}_r$(inter) of these materials also are predicted to be identical, as observed. Moreover, the associated homogeneous contributions to the linewidths are $\sigma_d \sim 0.3$ eV. Since this value is much smaller than the predicted inhomogeneous static-fluctuation-induced value $\sigma_s \simeq E_{re}(\text{inter})/2 = 0.75$ eV, we expect the observed UPS lines to be inhomogeneously broadened and about the same width in both PS and PVP, again in accordance with the measurements. The quantitative prediction of the experimental results by the model also is

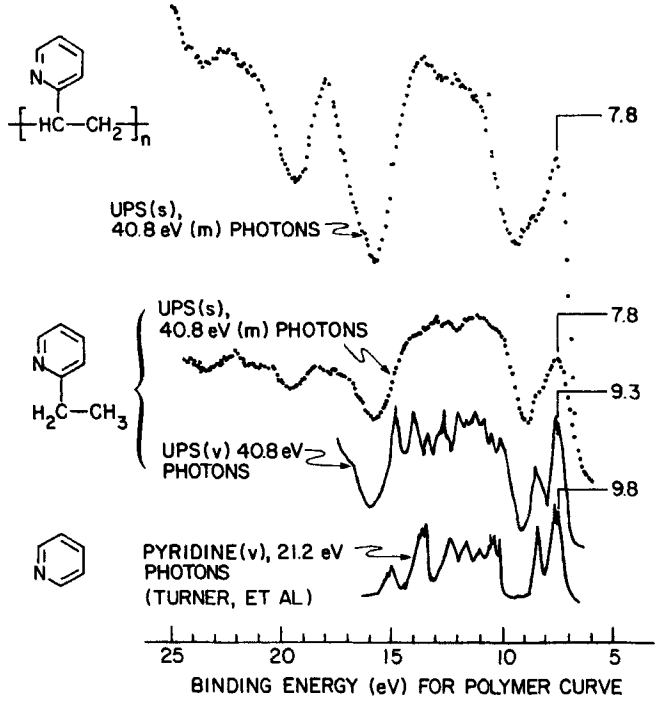

FIGURE 9 UPS data series of materials pyridine(v),[50] 2-ethyl pyridine(v), 2-ethyl pyridine(s), and poly(2-vinyl pyridine)(s). The shift of 0.5 eV between the lowest-binding energy peak for pyridine and for 2-ethyl pyridine reflects the effects of hyperconjugation induced by the ethyl group substituent. The additional shift of 1.5 eV between the vapor(v) and solid-state(s) data on 2-ethyl pyridine arises from the intermolecular relaxation effects discussed in the text. The spectra are presented in the figure shifted relative to each other by an amount such that the lowest-energy ionization potentials are aligned. The absolute values of these ionization potentials are indicated in the figure. [After Duke *et al.*[11]]

excellent,[11] although a more detailed consideration of this topic lies beyond the scope of the present paper.

The analysis of localization in molecular solids given by Duke[9] further predicted band-like motion in the segregated stack linear-chain charge transfer salts (because $\Delta \lesssim \bar{V}$) and a transition from hopping to band-like motion in Van der Waals crystals with decreasing temperatures below $T \simeq 100°K$ (because $\Delta \sim cT^{1/2}$). The former prediction was in accord with certain data available at that time,[13] and subsequently has been buttressed still further.[8,14] The latter phenomenon had not been observed previously, but subsequently this prediction also has been verified for naphthalene.[7] Therefore all of the expectations based on Eqs. (14) and (15) together with our earlier[9] theoretical estimates of Δ, ΔV, and $\bar{V}$ for molecular solids have been borne out by subsequent experimental measurements.

SYNOPSIS

In a series of earlier papers[3,9,10] a model of electronic states in molecular solids was proposed in which the localized or extended nature of these states results from a competition between site-energy fluctuations (induced by relaxation-energy fluctuations) and electron (or exciton) transfer integrals. This model, described by Eqs. (8), (14) and (15) herein, was applied to examine the microscopic nature of the states of charges injected into several types of molecular solids, specifically segregated-stack, linear chain charge transfer salts, Van der Waals crystals, and pendant-group and molecularly-doped polymers. The parameters characteristic of the model were estimated and several previously unnoticed phenomena (e.g., polarization-fluctuation-induced surface states, molecular-ion states in pendant-group polymers) were predicted. In the present paper we have reviewed extensions of this model to include dynamic as well as static relaxation-energy fluctuations and more recent experimental tests of the model's predictions. All of the new phenomena predicted[9] by the model subsequently have been observed.[7,11,12] Moreover, in those cases in which the model and its extensions could be tested quantitatively[11,12] it has proven adequate to describe the measurements. We argue, therefore, that this model provides a useful perspective from which to view the microscopic character of electronic states in molecular solids.

Acknowledgments

The author is indebted to L. J. Kennedy for assistance with the manuscript, to W. R. Salaneck for permission to use Fig. 6, to M. M. Shahin for his continuing support and encouragement of this work, and to W. H. H. Gunther and R. Bigelow for comments on the manuscript.

References

1. E. P. Goodings, *Chem. Soc. Revs.*, **5**, 95 (1976).
2. H. J. Wintle, *IEEE Trans. Elect. Insulation*, **12**, 97 (1977).
3. C. B. Duke and T. J. Fabish, *Phys. Rev. Lett.*, **37**, 1075 (1976).
4. T. J. Fabish and C. B. Duke, *J. Appl. Phys.*, **48**, 4256 (1977).
5. L. B. Schein, *Phys. Rev. B*, **15**, 1024 (1977).
6. L. B. Schein, *Chem. Phys. Lett.*, **48**, 571 (1977).
7. L. B. Schein, C. B. Duke and A. R. McGhie, *Phys. Rev. Lett*, **40**, 197 (1978).
8. A. J. Epstein and E. M. Conwell, *Solid State Commun.*, **24**, 627 (1977).
9. C. B. Duke, *Surface Sci*, **70**, 674 (1978).
10. C. B. Duke, T. J. Fabish and A. Paton, *Chem. Phys. Lett.*, **49**, 4256 (1977).
11. C. B. Duke, W. R. Salaneck, T. J. Fabish, J. J. Ritsko, H. R. Thomas and A. Paton, *Phys. Rev. B*, **18**, Dec. 15 (1978).
12. W. R. Salaneck, *Phys. Rev. Lett.*, **40**, 60 (1978).
13. A. J. Epstein, E. M. Conwell, D. J. Sandman and J. S. Miller, *Solid State Commun.*, **23**, 355 (1977).
14. E. M. Conwell, *Phys. Rev. Lett.*, **39**, 777 (1977); *Phys. Rev. B* (to be published).
15. N. O. Lipari and C. B. Duke, *J. Chem. Phys.*, **63**, 1748 (1975); **63**, 1768 (1975).

16. C. B. Duke, N. O. Lipari, W. R. Salaneck and L. B. Schein, *J. Chem. Phys.*, **63**, 1758 (1975).
17. K. L. Yip, N. O. Lipari, C. B. Duke, B. S. Hudson and J. Diamond, *J. Chem. Phys.*, **64**, 4020 (1976).
18. C. B. Duke, K. L. Yip, G. P. Ceasar, A. W. Potts and D. G. Streets, *J. Chem. Phys.*, **66**, 256 (1977).
19. K. L. Yip, C. B. Duke, W. R. Salaneck, W. R. Plummer and G. Loubriel, *Chem. Phys. Lett.*, **49**, 530 (1977).
20. W. R. Salaneck, J. W-p. Lin, A. Paton, C. B. Duke and G. P. Ceasar, *Phys. Rev. B*, **13**, 4517 (1976).
21. W. R. Salaneck, C. B. Duke, A. Paton, C. Griffiths and R. C. Keezer, *Phys. Rev. B*, **15**, 1100 (1977).
22. K. Wittel and S. P. McGlynn, *Chem. Rev.*, **77**, 745 (1977).
23. L. S. Cederbaum and W. Domcke, *Adv. Chem. Phys.*, **36**, 205, (1977).
24. R. Boschi and W. Schmidt, *Inorg. Nucl. Chem. Lett.*, **9**, 643 (1973).
25. P. Nielsen, *Phys. Rev. B*, **10**, 1673 (1974).
26. F. J. Himpsel, N. Schwenter and E. E. Koch, *Phys. Stat. Sol. (b)*, **71**, 615 (1975).
27. C. B. Duke, W. R. Salaneck, A. Paton, K. S. Liang, N. O. Lipari and R. Zallen, in *Structure and Excitations of Amorphous Solids*, G. Lucovsky and F. L. Galeener, eds. (American Institute of Physics, New York, 1976), pp. 23–30.
28. C. B. Duke and K. L. Yip, *Bull. Am. Phys. Soc.*, **22**, 399 (1977).
29. K. L. Yip and C. B. Duke, *Bull. Am. Phys. Soc.*, **22**, 399 (1977).
30. W. R. Salaneck, N. O. Lipari, A. Paton, R. Zallen and K. S. Liang, *Phys. Rev. B*, **12**, 1493 (1975).
31. N. O. Lipari, P. Nielsen, J. J. Ritsko, A. J. Epstein and D. J. Sandman, *Phys. Rev.*, **14**, 2229 (1976).
32. N. O. Lipari, C. B. Duke, R. Bozio, A. Girlando, C. Pecile and A. Padva, *Chem. Phys. Lett.*, **44**, 236 (1976).
33. N. O. Lipari, M. J. Rice, C. B. Duke, R. Bozio, A. Girlando and C. Pecile, *Int. J. Quant. Chem.*, **11**, 583 (1977).
34. C. B. Duke, N. O. Lipari and L. Pietronero, *Chem. Phys. Lett.*, **30**, 415 (1975); *J. Chem. Phys.*, **65**, 1165 (1976).
35. C. B. Duke and N. O. Lipari, *Chem. Phys. Lett.*, **36**, 51 (1975).
36. G. Varsanyi, *Vibrational Spectra of Benzene Derivatives* (Academic Press, New York, 1969).
37. C. B. Duke and G. D. Mahan, *Phys. Rev. A*, **139**, 1965 (1965).
38. C. B. Duke, in *Synthesis and Properties of Low-Dimensional Materials*, J. S. Miller and A. J. Epstein, eds. (New York Academy of Sciences, New York, 1978), pp. 166–178.
39. E. Lindholm, *Farad. Disc. Chem. Soc.*, **54**, 200 (1972).
40. A. W. Potts, W. C. Price, D. G. Streets and T. A. Williams, *Farad. Disc. Chem. Soc.*, **54**, 168 (1972).
41. M. D. Newton, *J. Phys. Chem.*, **79**, 2795 (1975).
42. C. B. Duke, in *Tunneling in Biological Systems*, B. Chance, ed. (Academic Press, New York, 1978), in press.
43. T. F. Soules and C. B. Duke, *Phys. Rev. B*, **3**, 262 (1971).
44. R. J. Elliot, J. A. Krumhansl and P. L. Leath, *Rev. Mod. Phys.*, **46**, 465 (1974).
45. D. Weaire and A. R. Williams, *J. Phys. C*, **10**, 1239 (1977).
46. D. Weaire and V. Srivastava, in *Amorphous and Liquid Semiconductors*, W. E. Spear, ed. (G. G. Stevenson Ltd., Dundee, 1977), pp. 286–290.
47. E. N. Economon and P. D. Antoniou, *Solid State Commun.*, **21**, 285 (1977).
48. I. Ikemoto, K. Samizo, T. Fujikawa, K. Ishii, T. Ohta and H. Kuroda, *Chem. Lett.*, 758 (1974).
49. R. Boschi, J. N. Murrell and W. Schmidt, *Farad. Disc. Chem. Soc.*, **54**, 116 (1972).
50. D. W. Turner, C. Baker, A. D. Baker and C. R. Brundle, *Molecular Photoelectron Spectroscopy* (Wiley Interscience, London, 1970), p. 271, 332.